RADAR-BASED STOCHASTIC PRECIPITATION NOWCASTING USING THE SHORT-TERM ENSEMBLE PREDICTION SYSTEM (STEPS) (CASE STUDY: PANGKALAN BUN WEATHER RADAR)

Abdullah Ali[1,3]*, Supriatna[1], Umi Sa'adah[2]
[1]Universitas Indonesia, Department of Geography
[2]Jakarta Meteorological Watch Office BMKG
[3]Remote Sensing Data Management Division, Center for Public Weather Service, Indonesia Agency for Meteorology Climatology and Geophysics (BMKG)
*e-mail: abdullah.ali@ui.ac.id

Received: 24 January 2021; Revised: 18 May 2021; Approved: 1 June 2021

Abstract. Nowcasting, or the short-term forecasting of precipitation, is urgently needed to support the mitigation circle in hydrometeorological disasters. Pangkalan Bun weather radar is single-polarization radar with a 200 km maximum range and which runs 10 elevation angles in 10 minutes with a 250 meters spatial resolution. There is no terrain blocking around the covered area. The Short-Term Ensemble Prediction System (STEPS) is one of many algorithms that is used to generate precipitation nowcasting, and is already in operational use. STEPS has the advantage of producing ensemble nowcasts, by which nowcast uncertainties can be statistically quantified. This research aims to apply STEPS to generate stochastic nowcasting in Pangkalan Bun weather radar and to analyze its advantages and weaknesses. Accuracy is measured by counting the possibility of detection and false alarms under the 5 dBZ threshold and plotting them in a relative operating characteristic (ROC) curve. The observed frequency and forecast probability is represented by a reliability diagram to evaluate nowcast reliability and sharpness. Qualitative analysis of the results showed that the STEPS ensemble produces smoothed reflectivity fields that cannot capture extreme values in an observed quasi-linear convective system (QLCS), but that the algorithm achieves good accuracy under the threshold used, up to 40 minutes lead time. The ROC shows a curved upper left-hand corner, and the reliability diagram is an almost perfect nowcast diagonal line.

Keywords: *weather radar, nowcasting, Short Term Ensemble Prediction Systems (STEPS)*

1 INTRODUCTION

Hydrometeorological disasters are major natural disasters and have tended to increase in frequency in Indonesia over the last ten years (BNPB, 2020). They not only cause material loss but also claim lives. In the period 2009-2019, floods resulted in 2,308 deaths/missing people, 44,585 severely damaged houses, 712 damaged health facilities, 3,192 damaged religious facilities, and 5,926 damaged educational facilities (BNPB, 2020).

One of the main factors causing hydrometeorological disasters is extreme rainfall (Adi, 2013). An early warning system for extreme weather monitoring is needed to mitigate such disasters (Putri, 2018). Prediction information on extreme rainfall will provide an initial warning to decision-makers to proceed with urgent action. In addition, early warning rainfall systems can also be used to support the policies for protecting flood-prone areas. Therefore, an accurate early warning system of extreme rainfall is needed to minimize the costs of hydrometeorological disaster.

In terms of time span, weather prediction is divided into several types: very long range, long range, medium

http://dx.doi.org/10.30536/j.ijreses.2021.v18.a3527

range, and short range/nowcasting. The nowcasting process includes a detailed explanation of current weather conditions, together with predictions obtained from extrapolation up to the following 6 hours (WMO, 2020). The nowcasting process is closely related to the detection of convective cloud systems. Currently, the nowcasting process mostly uses weather radar for the principle data. Some of the main methods that have been developed include thunderstorm detection, tracking, and extrapolation (Xu, 2012), such as the centroid tracking method (Crane, 1979; Dixon & Wiener, 1993; Johnson et al., 1998); tracking radar echo by correlation (TREC) (Rinehart & Garvey, 1978; Wilson et al., 1998; Chen et al., 2007); and optical flow methods (Han, 2008). Compared to meteorological satellites, weather radar is able to make more detailed storm detection.

The centroid tracking method can only be used for convective precipitation systems, while TREC can also be employed in precipitation systems with layered clouds. When TREC is used in a rapidly changing convective precipitation system, the error rate increases significantly (Cao et al., 2015). Optical flow is a vector displacement in a dense plane that defines the transition of each pixel in a region. The method is calculated using a brightness constraint, with the assumption of brightness constancy for each pixel in a sequential frame. Optical flow is therefore commonly used as a feature in segmentation based on movement and tracking applications (Yilmaz et al., 2006). This advantage can overcome the drawbacks of centroid tracking and TREC methods. However, the level of success of the optical flow method is limited because it does not consider the physical implication of the development of radar echoes. Therefore, predicting local-scale convection systems that are rapidly evolving or extending is very difficult.

Several nowcasting systems that are already operational in various countries (Woo & Wong, 2017; Pulkkinen, 2020) include:

1. Spectral Prognosis (S-PROG), developed by the Bureau of Meteorology (BoM), Australia.
2. Short-Term Ensemble Prediction Systems (STEPS), a result of cooperation between UKMO and BoM, UK and Australia.
3. Auto Nowcasting System (ANC), used by the National Center of Atmospheric Research (NCAR), United States.
4. McGill Algorithm for Precipitation Nowcasting Using Semi-Lagrangian Extrapolation (MAPLE), developed by McGill University, Canada.
5. Short-range Warning of Intense Rainstorms in Localized Systems (SWIRLS), produced by the Hongkong Observatory, Hong Kong.
6. Dynamic and adaptive radar tracking of storms (DARTS), developed by CASA Dallas-Forth Worth.
7. String of Beads Model for Nowcast (SBMcast), used by the Spanish Meteorology Agency (AEMET) and the Catalan Weather Service (SMC).

Several algorithms have also been developed for precipitation nowcasting but are still at the research stage, such as Scale Filtering DARTS (SF-DARTS); Vertically Integrated Liquid Based Nowcasting (RadVil); Autoregressive Nowcasting Using VIL (ANVIL); and Lagrangian Persistence (LP-R). In Indonesia, BMKG, which operates 42 weather radars, applied the MAPLE algorithm during the period 2009-2018, as provided by Weather Decision Technologies (WDT). After the license expired in 2018, there are no nowcasting products using weather radar data.

In this research, the STEPS algorithm was chosen to generate

precipitation nowcasting using BMKG weather radar data, due to its proven good performance (Pulkkinen, 2018), and as it is already at the operational stage. The algorithm was developed based on S-PROG, with the addition of stochastic perturbation into the reflectivity and advection fields to generate the ensemble nowcast. Another advantage of such nowcasting is its capability to compute uncertainties statistically.

2 MATERIALS AND METHODOLOGY

2.1 Pangkalan Bun Weather Radar

The study used non-polarimetric C-Band weather radar with a 200 km maximum range, 250 m spatial resolution, and nine elevation angles. Figures 2-1 and 2-2 show the radar scanning strategy and beam blockage analysis. The scanning strategy was optimised to enable dense observation at a low elevation in order to maximise precipitation detection. The beam blockage analysis shows that there was no blocking due to topography in any direction. Because of these two aspects, the radar should theoretically produce good data. The radar hardware specification is shown in Table 2-1.

2.2 Study area

The study area covered 200 km around the Pangkalan Bun radar point location, including both land and the northern part of the Java Sea, so that cloud systems growing and developing over the land or sea would be detected. The extreme rainfall that occurred on January 28-29, 2018 (BMKG Pangkalan Bun report, 2018) due to quasi-linear convective system (QLCS) was used to evaluate the accuracy of the STEPS algorithm.

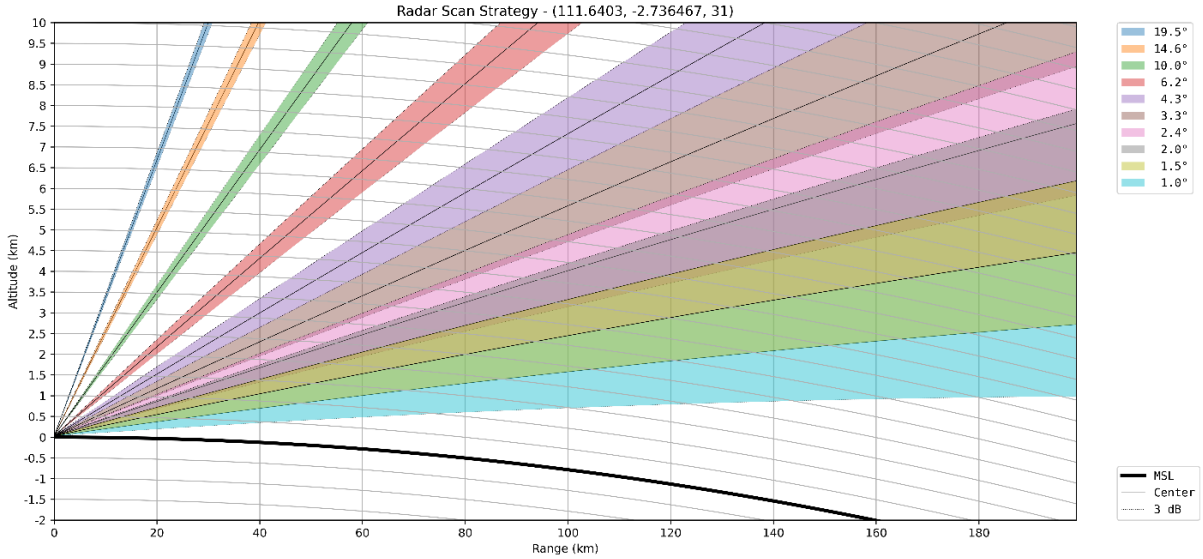

Figure 2-1: Pangkalan Bun weather radar scanning strategy

Table 2-1: Radar hardware specification

Parameter	Value
Radar site name	Pangkalan Bun
Latitude	-2.736467° S
Longitude	111.6403° E
Altitude	31 m
Tower height	20 m
Frequency	5.6 GHz
Beam width	<1°
Pulse width	0.5 - 2.0 µs
PRF Min	250 Hz
PRF Max	1200 Hz
Signal Processor	GDRX-SP
Transmitter Type	Coaxial magnetron
Polarization	Single
Installation year	2014
Manufacturer	Selex SI GmBH

2.2 Study area

The study area covered 200 km around the Pangkalan Bun radar point location, including both land and the northern part of the Java Sea, so that cloud systems growing and developing over the land or sea would be detected. The extreme rainfall that occurred on January 28-29, 2018 (BMKG Pangkalan Bun report, 2018) due to quasi-linear convective system (QLCS) was used to evaluate the accuracy of the STEPS algorithm.

2.3 Methods

The stochastic precipitation nowcasting methodology used in the research is based on the work of Bowler et al. (2006). The fundamental assumption is that the structure and intensity of rainfall can be described by the multiplicative cascade model and lognormal distribution, an approach that is described in detail by Kedem and Chiu (1987) and Veneziano et al. (1996). Due to this assumption, the reflectivity field in the dBZ units at time *t*, which corresponds to the logarithm of rain rate, can be decomposed into an additive cascade:

$$Z_{i,j}(t) = \sum_{k=1}^{n} \sigma_k(t) Y_{k,i,j}(t) + \mu_k(t) \quad (2\text{-}1)$$

where each cascade level k represents a certain spatial scale. $Y_{k,i,j}$ is a random variable having the standard normal distribution after normalisation by the mean μ_k and standard deviation σ_k, while i and j denote the spatial coordinates. That above decomposition was obtained by applying a fast Fourier transform (FFT) and Gaussian band-pass filter sequence to the reflectivity field *Z(t).*

The lead time is denoted by t_l, the forecast reflectivity field by $\hat{Y}_k\ (t+ t_l)$, and the cascade level k is given by the weighted sum:

$$\hat{Y}_k(t + t_l) = w_k^e(t + t_l)\, Y_{k.i.j}^e(t + t_l) + w_k^n(t + t_l)\, Y_{k.i.j}^n(t + t_l) \quad (2\text{–}2)$$

where the weights w_k^e and w_k^n are formulated by:

$$w_k^e(t + t_l) = \rho_k(t + t_l)$$
$$w_k^n(t + t_l) = \sqrt{1 - w_k^e(t + t_l)^2} \quad (2\text{-}3)$$

The model for the temporal evolution of the reflectivity field consists of two complementary cascades: the extrapolation (Y_k^e) and noise (Y_k^n) cascades. These two variables are governed by autoregressive (AR2) models:

$$Y_{k,i,j}^e(t + t_l) = \phi_{k,1} Y_{k,i,j}^e(t + t_l - \Delta t) + \phi_{k,2} Y_{k,i,j}^e(t + t_l - 2\Delta t) \quad (2\text{-}4)$$

$$Y_{k,i,j}^n(t + t_l) = \phi_{k,1} Y_{k,i,j}^n(t + t_l - \Delta t) + \phi_{k,2} Y_{k,i,j}^n(t + t_l - 2\Delta t) + \phi_{k,0} \varepsilon_{k,i,j}(t + t_l) \quad (2\text{-}5)$$

$$\rho_k(t + t_l) = \phi_{k,1}\, \rho_k(t + t_l - \Delta t) + \phi_{k,2}\, \rho_k(t + t_l - 2\Delta t) \quad (2\text{-}6)$$

$$\rho_k(t + \Delta t) = \rho_{k,1}(t);\ \rho_k(t + 2\Delta t) = \rho_{k,2}(t) \quad (2\text{-}7)$$

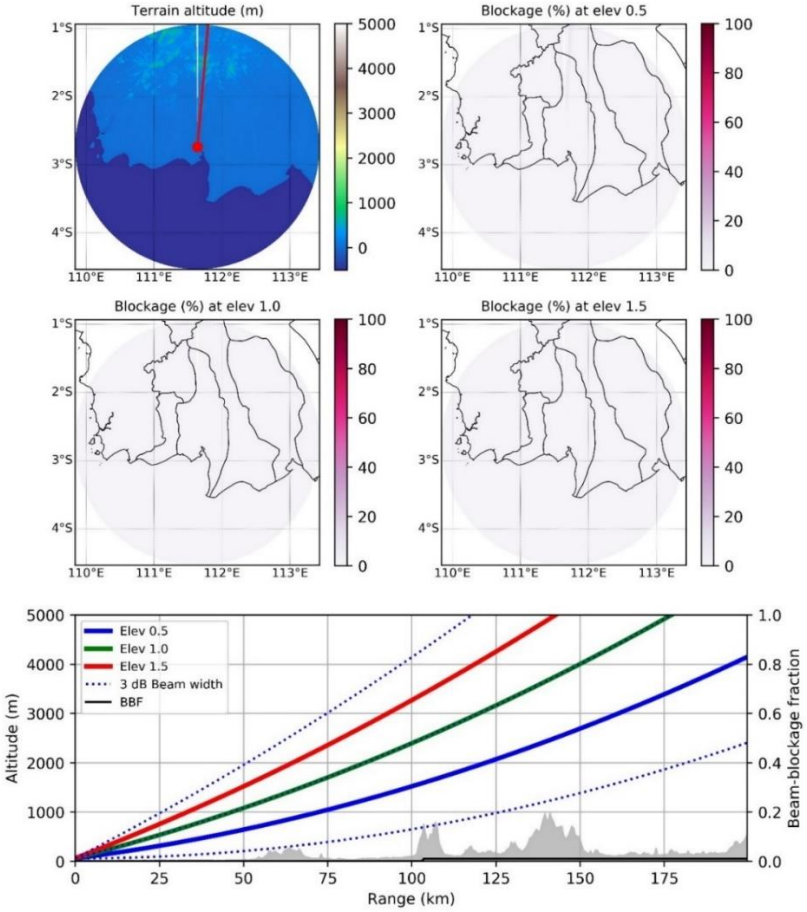

Figure 2-2: Pangkalan Bun beam blockage analysis. There is no terrain blocking in any direction.

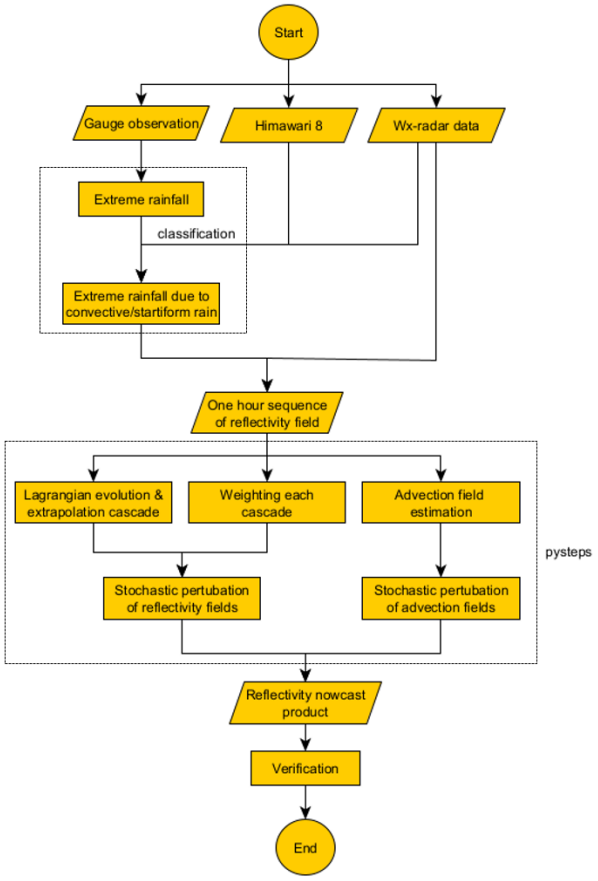

Figure 2-3: Research flowchart

where autocorrelation $\rho_k(t + t_l)$ represents the explained variance; and Δt denotes the time step between the consecutive reflectivity radar data (t_l is assumed as a multiple of Δt). The parameters $\phi_{k,1}$and $\phi_{k,2}$were obtained from the initial lag-1 and lag-2 autocorrelation coefficients:

$$\phi_{k,1} = \frac{\rho_{k,1}(t)[1 - \rho_{k,2}(t)]}{1 - \rho_{k,1}(t)^2} \quad (2\text{-}8)$$

$$\phi_{k,2} = \frac{\rho_{k,2}(t)[1 - \rho_{k,1}(t)]}{1 - \rho_{k,1}(t)^2} \quad (2\text{-}9)$$

The perturbation fields added to the noise cascade levels (Y_k^n) at each iteration step are denoted by $\varepsilon_{k,i,j}$. All the equations to generate the nowcasting were executed using the pysteps Python package (Pulkkinen et al., 2019). The comprehensive steps are shown in the flowchart in Figure 2-3.

3 RESULTS AND DISCUSSION

The extreme weather that occurred in Pangkalan Bun on 28-29 January 2018 was reported by a synop report and also captured by Himawari 8 natural colour and enhanced infrared imagery (Figure 3-1).

The single polarization weather radar of Pangkalan Bun operates with a temporal resolution of 10 minutes. The radar reflectivity input data used was a product of CMAX (Column Maximum), which is the maximum value of all elevations in a column. CMAX products were used based on the research conducted by Ali et al. (2019), in which the best rainfall estimate was obtained from these products. In contrast, Pulkkinen's (2018) research used CAPPI products from the 4th lowest elevations of weather radar observations for the input data of the reflectivity fields.

When a single deterministic nowcast is desired from a STEPS ensemble, the ensemble mean can be considered as the best estimate (Pulkkinen, 2018). The number of ensemble members used for this study was 20, dues to hardware limitations. In Pulkkinen's (2020) research, the number of ensembles was not linear with the accuracy of the model. A model value with a greater number of ensemble members (96) is no better than with 48 members. The threshold value used was 5 dBZ, which gives a non-zero precipitation estimation.

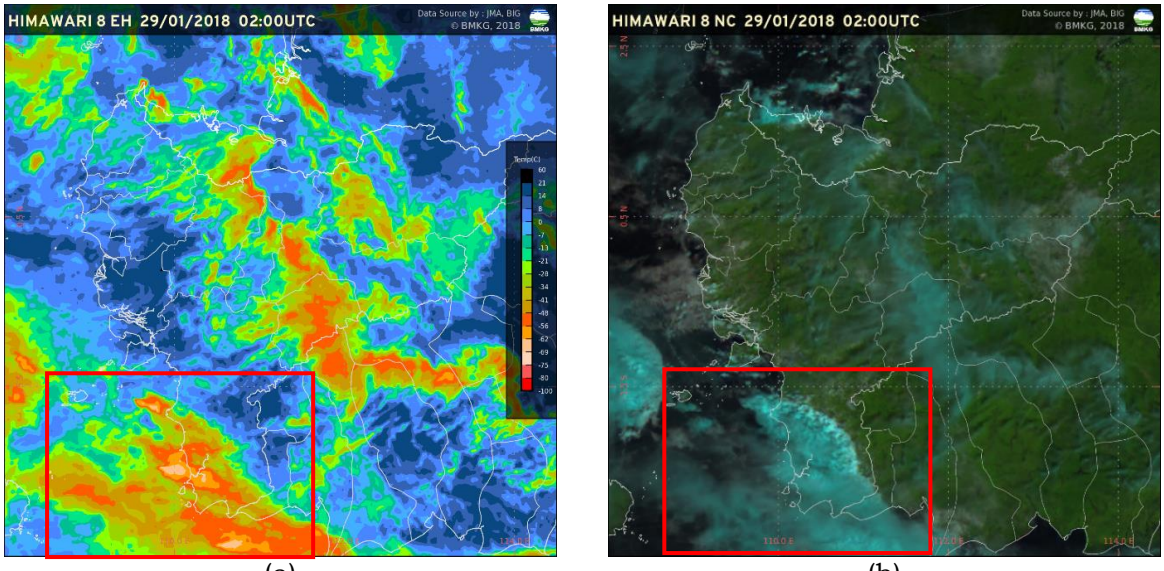

(a) (b)

Figure 3-1: (a) Enhanced infrared and (b) natural colour Himawari 8 imagery that captures the extreme weather occurence in Pangkalan Bun.

The results of a qualitative comparison of the probabilistic nowcasts are shown in Figure 3-2. The STEPS ensemble provided smoothed reflectivity fields that could not capture the extreme values in a quasi-linear convective system (QLCS), which was a convective cloud system lined up due to the cold pool (Ali, 2018). The STEPS algorithm also models the growth and decay processes (Bower, 2006), although in Figure 3-2 it is shown that the nowcast results tended to lead to the systems undergoing a decaying process, whereas the observations showed that the convective cloud system in the QLCS was still at mature stage.

The QLCS direction is well predicted by the model. The typical structure of QLCS, that is leading edge, is still predicted at a 10 minutes lead time, but it begins disappear at a 30 minutes lead time. It can be inferred that the advection field results a good movement prediction. Cloud propagation is predicted to move eastward, and the observation data also show eastward movement.

In this research, STEPS accuracy was evaluated with two kinds of curve: a relative operating characteristic (ROC) curve, and a reliability diagram. The ROC curve was used to evaluate the discriminatory power of the nowcast exceeding threshold used (5 dBZ) at a set of increasing probability threshold. In this case, the probability threshold used was 0.1 to 1 for ten steps. The ROC curve contained the probability of detection (POD) in the y-axis, against the false alarm rate (FAR) in the x-axis for the probability threshold. An ideal nowcast will result in a curve that passes through the upper left-hand corner, indicating that there exists a range of probability thresholds, from which one can obtain high detection probabilities, while also keeping the false alarm rate low (Jolliffe & Stephenson, 2003)

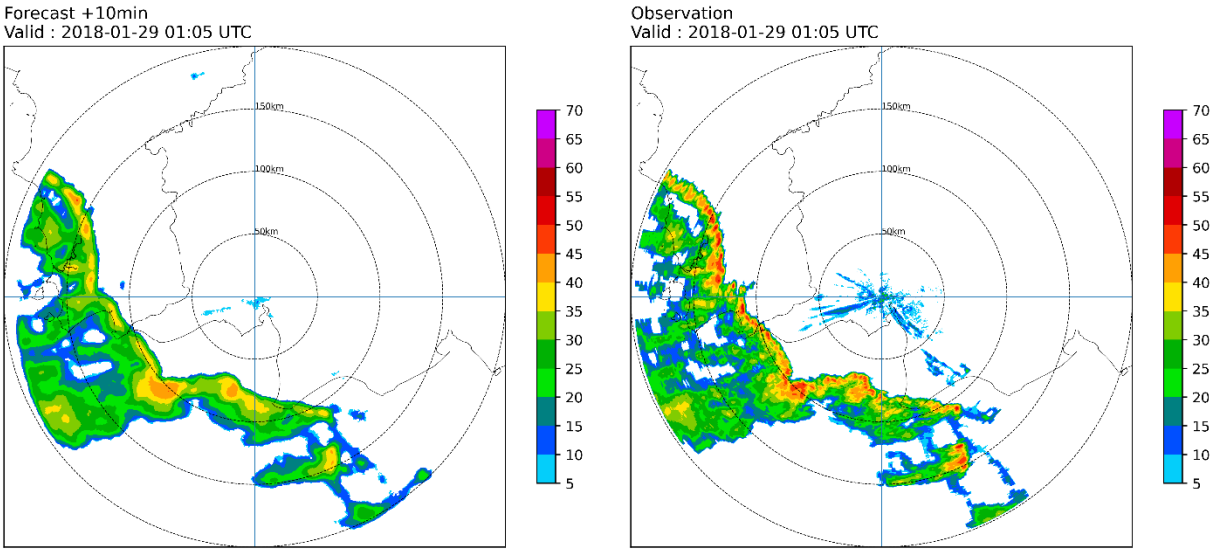

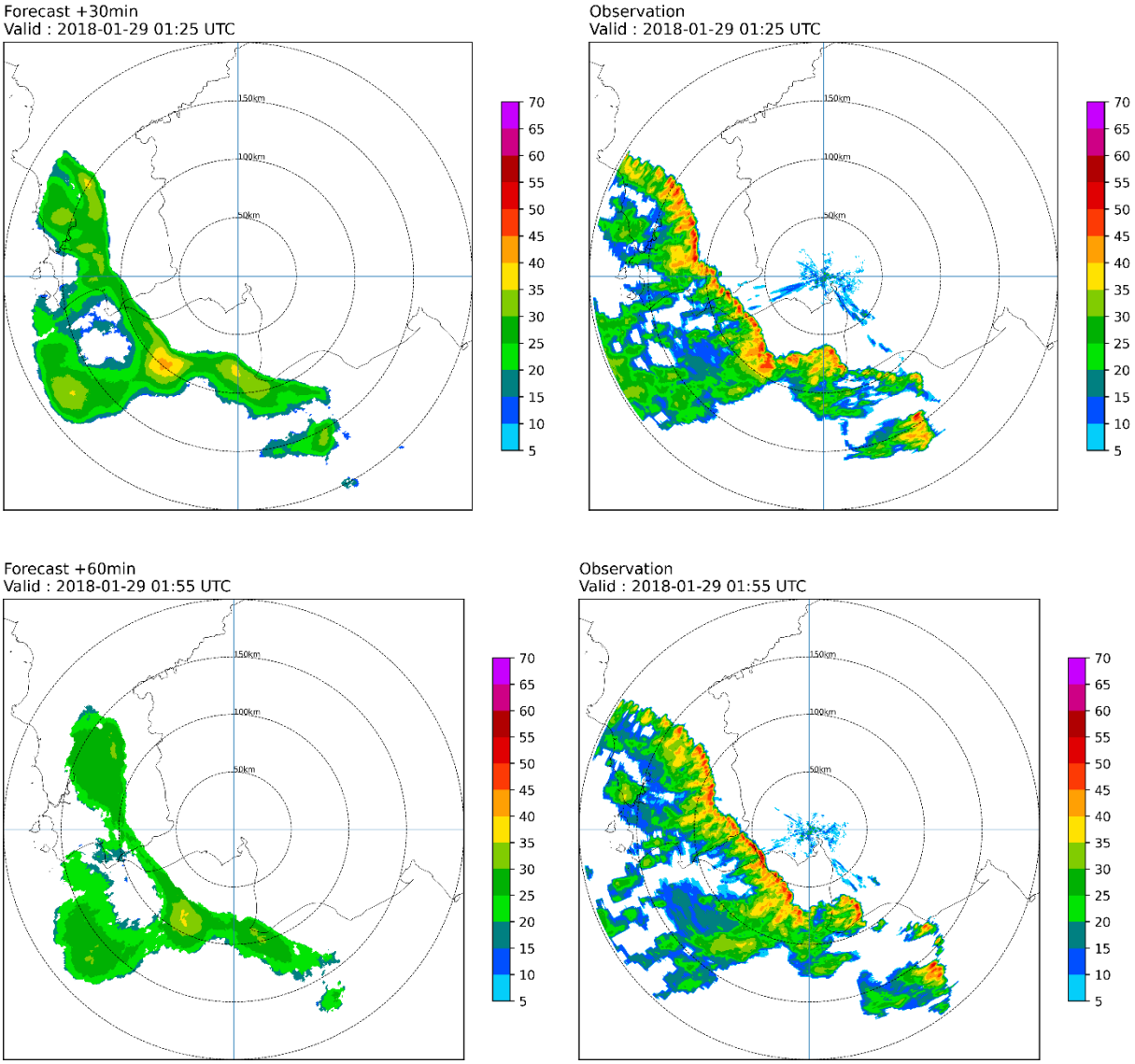

Figure 3-2: Qualitative comparison between the STEPS nowcast at 10-, 30-, and 60-minute lead times and the observation data at the same time. It can be seen that the pattern is similar, but extreme values could not be captured by STEPS due to its smoothing process.

Figure 3-3a and 3-3c shows the ROC curve and reliability diagram for 10-40 minute (a and b) and 1 hour (c and d) lead times for a given reflectivity threshold (5 dBZ). The ROC curve will give an appropriate probability threshold which has a maximum number of hits and minimum number of false alarms. It can be seen that the false alarm values are quite low, so the POFD value is less than 0.2, while the POD values for the 10-40 minutes lead times are greater than 0.7 (70%). These results indicate good STEPS nowcast skills with a 5 dBZ threshold. The area below the curve is also greater than 0.75 up to 40 minutes.

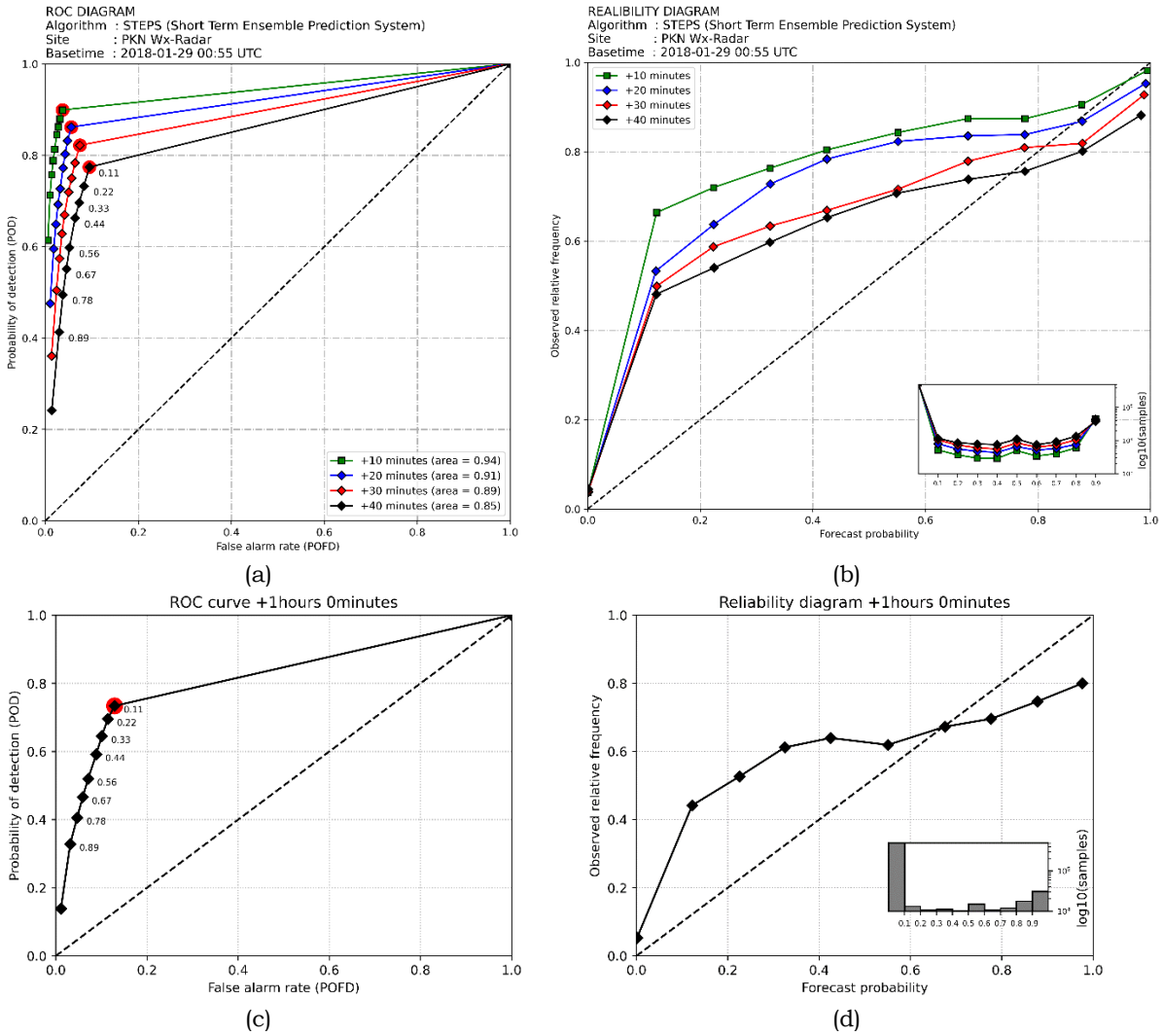

Figure 3-3: ROC curve and realibility diagram, 10-40 minute and 1 hour time steps.

The reliability diagram shows the observed frequencies of the reflectivity fields above the given threshold compared to the predicted probability (Bocker & Smith, 2007). The diagram was produced by dividing the probability interval between 0 to 1 into equally spaced bins. A perfectly reliable nowcast will give a diagonal curve, while a poor one will be under/above 0.4 diagonal line. Typically, a reliability diagram also contains a histogram of the sample size for each probability interval that represents the nowcast sharpness. For good sharpness, the predicted probabilities should be close to either 0 or 1.

Figure 3-3 shows the reliability diagram computed from the STEPS nowcast ensemble with the given threshold. The nowcasts are sharp for all the lead times up to 40 minutes. The curves approach closer to the diagonal line for increasing probability forecast values. The implication of the reliability diagram is that precipitation above the threshold is analysed, and STEPS gives reliable estimates of the probability of precipitation with lower reflectivity.

Besides the advantages of accommodating forecast uncertainty, and improved ensemble prediction by making lagged average forecasts (Miyakoda & Talagrand, 1971), there are also weaknesses in the nowcasting results, with the prediction results not able to capture extreme values. In Figure 3-2, it can be seen that the STEPS prediction results show a decreasing trend in intensity in line with increasing time steps. This might occur because there are

no special skills in generating perturbation STEPS; the generated perturbation is not simply random, but rather, based on the hidden dynamics at each time step.

4 CONCLUSION

Stochastic nowcasting was applied to Pangkalan Bun single polarization weather radar. The radar itself is directly adjacent to the Java Sea and Karimata Strait, so precipitation often approaches from the sea. The STEPS algorithm was used, which has the advantage of producing an ensemble nowcast, in which nowcast uncertainties can be statistically quantified. The input data of the STEPS algorithm comprised a one-hour sequence of latest weather radar reflectivity fields, then continued by Lagrangian evolution, cascading of the reflectivity, estimation of the advection field, and computation of the stochastic perturbation to the reflectivity field and advection field to produce the nowcasting product. Twenty ensemble members were used, and the mean value was verified with real observation at the same time using an ROC curve and reliability diagram.

The nowcasting product provided good accuracy for the 40 minutes lead time. The ROC showed an upper left-hand corner curve with more than 70% possibility of detection, less than 20% of false alarm, and with more than 75 % of the area below the curve. The algorithm can produce a reliable nowcast of up to 40 minutes with a 5 dBZ threshold. These results were encouraging for the first attempt.

Forecast uncertainty represented by the number of ensemble members is an advantage of this algorithm, and can be improved by a lagged ensemble forecast. Precipitation propagation, which is an important aspect of extreme weather warnings, can be predicted accurately. However, the prediction cannot capture extreme values. The tendency that occurs is a dissipating reflectivity field. Several aspects of the research need to be developed; for instance, evaluation of different thresholds in the case of testing model performance for different rainfall intensities. Another weakness is that the algorithm schema is quite complicated to apply.

There are several works that must be developed, for instance, evaluating different threshold in case of testing model performance for different rainfall intensities.

ACKNOWLEDGEMENTS

The research data were fully supported by the BMKG Weather Radar Data Management Sub Division. The paper was improved by the helpful suggestions of Dr. Hidde Leijnse from KNMI Netherland. The author wishes to thank all those who helped with the research.

AUTHOR CONTRIBUTIONS

Radar-Based Stochastic Precipitation Nowcasting Using The Short-Term Ensemble Prediction System (Steps) (Case Study: Pangkalan Bun Weather Radar). Lead author: Abdullah Ali. Co-Author: Supriatna, Umi Sa'adah. Author contributions are as follows:

1. Abdullah Ali: Weather radar and satellite image processing, STEPS nowcasting modelling, map layouting, results analysis
2. Supriatna: Provision of introduction
3. Umi Sa'adah: Provision of weather radar data and prepare draft manuscript

REFERENCES

Adi, S. (2013). Karakterisasi Bencana Banjir Bandang. Jurnal Sains dan Teknologi Indonesia, 15(1), 42-51.

Ali, A., Adrianto, R., & Saepudin, M. (2019). Preliminary Study of Horizontal And Vertical Wind Profile Of Quasi-Linear

Convective Utilizing Weather Radar Over Western Java Region, Indonesia. International *Journal of Remote Sensing and Earth Sciences (IJReSES), 15*(2), 177-186.

Ali, A., Deranadyan, G., & Umam, I. H. (2020). An Enhancement to The Quantitative Precipitation Estimation Using Radar-Gauge Merging. *International Journal of Remote Sensing and Earth Sciences (IJReSES), 17*(1), 65-74.

Bowler, N. E., Pierce, C. E., & Seed, A. W. (2006). STEPS: A probabilistic precipitation forecasting scheme which merges an extrapolation nowcast with downscaled NWP. *Quarterly Journal of the Royal Meteorological Society: A Journal of the Atmospheric Sciences, Applied Meteorology and Physical Oceanography, 132*(620), 2127-2155.

Bröcker, J., & Smith, L. A. (2007). Increasing the eliability of reliability diagrams. *Weather and Forecasting, 22*(3), 651-661.

Cao, C. Y., Chen, Y. Z., Liu, D. H., Li, C., Li, H., & He, J. (2015). The optical flow method and its application to nowcasting. *Acta Meteor. Sinica*, *73*, 471-480.

Chen, M. X., Wang, Y. C., & Yu, X. D. (2007). Improvement and application test of TREC algorithm for convective storm nowcast. *J. Appl. Meteor. Sci, 18*, 690-701.

Crane, R. K. (1979). Automatic cell detection and tracking. *IEEE Transactions on Geoscience Electronics, 17*(4), 250-262.

Dixon, M., & Wiener, G. (1993). TITAN: Thunderstorm identification, tracking, analysis, and nowcasting—A radar-based methodology. *Journal of Atmospheric and Oceanic Technology, 10*(6), 785-797.

Han, L., Wang, H. Q., & Lin, Y. J. (2008). Application of optical flow method to nowcasting convective weather. *Acta Scientiarum Naturalium Universitatis Pekinensis, 44*(5), 751-755.

Johnson, J. T., MacKeen, P. L., Witt, A., Mitchell, E. D. W., Stumpf, G. J., Eilts, M. D., & Thomas, K. W. (1998). The storm cell identification and tracking algorithm: An enhanced WSR-88D algorithm. *Weather and Forecasting, 13*(2), 263-276.

Jolliffe, I. T., & Stephenson, D. B. (2003). *Forecast Verification: A Practitioner's Guide in Atmospheric Science*. John Wiley and Sons.

Kedem, B., & Chiu, L. S. (1987). On the lognormality of rain rate. *Proceedings of the National Academy of Sciences, 84*(4), 901-905.Miyakoda, K., & Talagrand, O. (1971). The assimilation of past data in dynamical analysis. *I. Tellus, 23*(4-5), 310-317.

Pulkkinen, S., Chandrasekar, V., & Harri, A. M. (2018). Nowcasting of precipitation in the high-resolution Dallas–Fort Worth (DFW) urban radar remote sensing network. *IEEE Journal of Selected Topics in Applied Earth Observations and Remote Sensing, 11*(8), 2773-2787

Pulkkinen, S., Chandrasekar, V., von Lerber, A., & Harri, A. M. (2020). Nowcasting of convective rainfall using volumetric radar observations. IEEE Transactions on Geoscience and Remote Sensing, 58(11), 7845-7859.

Putri, Y. P. (2018). Arahan Kebijakan Mitigasi Bencana Banjir Bandang di Daerah Aliran Sungai (DAS) Kuranji, Kota Padang. *Majalah Ilmiah Globe, 20*(2), 87-98.

Rinehart, R. E., & Garvey, E. T. (1978). Three-dimensional storm motion detection by conventional weather radar. *Nature, 273*(5660), 287-289.

Veneziano, D., Bras, R. L., & Niemann, J. D. (1996). Nonlinearity and self-similarity of rainfall in time and a stochastic model. *Journal of Geophysical Research: Atmospheres, 101(D21)*, 26371-26392.

Wilson, J. W., Crook, N. A., Mueller, C. K., Sun, J., & Dixon, M. (1998). Nowcasting thunderstorms: A status report. *Bulletin of the American Meteorological Society, 79*(10), 2079-2100.

Woo, W. C., & Wong, W. K. (2017). Operational application of optical flow techniques to radar-based rainfall nowcasting. *Atmosphere, 8*(3), 48.

Yilmaz, A., Javed, O., & Shah, M. (2006). Object tracking: A survey. *ACM Computing Surveys (CSUR), 38*(4), 13-es.

Yu, X. D., Zhou, X. G., & Wang, X. M. (2012). The advances in the nowcasting techniques on thunderstorms and severe convection. *Acta Meteorologica Sinica, 70*(3), 311-3